Research Square

Preprints are preliminary reports that have not undergone peer review.
They should not be considered conclusive, used to inform clinical practice,
or referenced by the media as validated information.

Fractional-Order Modeling of Ebola Virus Transmission: Stability Analysis and Numerical Simulations

S. Kosari

s.kosari@sutech.ac.ir

Shiraz University of Technology

M. H. Heydari

Shiraz University of Technology

D. Baleanu

Lebanese American University

M. Bayram

Biruni University

Article

Keywords: Ebola disease, Asymptotic stability, Lyapunov-Caputo sense, Fractional epidemic model, Caputo fractional derivative, Generalized hat functions

Posted Date: June 4th, 2026

DOI: https://doi.org/10.21203/rs.3.rs-9731192/v1

License: This work is licensed under a Creative Commons Attribution 4.0 International License.
Read Full License

Additional Declarations: No competing interests reported.

Fractional-Order Modeling of Ebola Virus Transmission: Stability Analysis and Numerical Simulations

S. Kosari*[1,2], M. H. Heydari[1], D. Baleanu[3], M. Bayram[4]

[1] *Department of Mathematics, Shiraz University of Technology, Shiraz, Iran.*

[2] *Department of Mathematics, University of Zabol, Zabol, Iran.*

[3] *Department of Computer Science and Mathematics, Lebanese American University, Beirut, 13-5053, Lebanon.*

[4] *Department of Computer Engineering, Biruni University, Istanbul, Turkey.*

Abstract

This paper develops a fractional-order Caputo model for Ebola virus disease using a six-compartment $SEIHFR$ framework that explicitly incorporates hospitalization and post-mortem transmission. We derive the basic reproduction number $\mathcal{R}_0$, prove local and global asymptotic stability of both disease-free and endemic equilibria using Routh-Hurwitz-Caputo criteria and Lyapunov functions, and perform sensitivity analysis to identify key transmission parameters. Numerical simulations employing generalized hat functions demonstrate that the fractional order ℓ modulates outbreak speed and memory effects without altering equilibrium stability. The results quantify how interventions such as safe burial, hospitalization, and contact reduction influence outbreak dynamics. A sufficient condition $\eta_H\gamma_F \geq \eta_F\gamma_{DH}$ is derived and interpreted epidemiologically as a balance between hospital infection control and burial efficacy. This study provides the first complete global stability analysis for a fractional $SEIHFR$ Ebola model and establishes a rigorous theoretical foundation for memory-aware outbreak response planning.

Keywords: Ebola disease; Asymptotic stability; Lyapunov-Caputo sense; Fractional epidemic model; Caputo fractional derivative; Generalized hat functions.

1. Introduction

Investigating Ebola is critical due to its high fatality rate, rapid transmission, and potential to cause severe public health crises and sociology-economic disruption. This study contributes by developing a fractional-order Caputo model that captures memory effects and real-world dynamics more accurately than classical models. It provides a detailed stability analysis of equilibrium points and calculates sensitivity indices to identify key intervention parameters. The numerical solution using generalized hat functions offers a reliable computational

*Corresponding author

Email address: s.kosari@sutech.ac.ir, sajad.kosari@uoz.ac.ir, heydari@sutech.ac.ir, dumitru.baleanu@lau.edu.lb, mustafabayram@biruni.edu.tr (S. Kosari*[1,2], M. H. Heydari[1], D. Baleanu[3], M. Bayram[4])

approach for simulating outbreak scenarios. These insights can directly inform containment strategies and optimize control measures during outbreaks. Ebola disease is a severe, often fatal illness caused by infection with Ebola viruses, which belong to the family of viral hemorrhagic fevers. It is named after the Ebola River in the Democratic Republic of the Congo, formerly Zaire. Primates, including monkeys and humans, can contract the Ebola virus. It spreads through direct contact with infected animals' bodily fluids. The virus has five species, Bundibugyo, Zaire, Reston, Sudan, and Taiforest [1]. People contract this virus primarily through direct exposure between broken skin and infected blood. Based on the latest 2014 outbreak in West Africa, interaction with recently deceased Ebola victims accounted for approximately 30 per cent of transmissions [1]. The disease typically begins suddenly with symptoms appearing 2 to 21 days after exposure, most commonly around 8 to 10 days. Early symptoms, often called dry symptoms, include, fever, severe headache, muscle, joint pain, weakness, fatigue and sore throat. As the disease progresses, after about 4 to 5 days, wet symptoms may develop, including, loss of appetite, nausea and vomiting, diarrhea, abdominal pain, unexplained bleeding from mucous membranes, skin, eyes, or internal organs, and other symptoms such as chest pain, shortness of breath, confusion, red eyes, rash, hiccups, and seizures. Survivors may experience long-term complications such as fatigue, headaches, muscle and joint pain, eye problems, like blurry vision, pain, redness, memory loss, depression, and other neurological symptoms. Ebola has a high fatality rate, ranging from 25 to 90 percent depending on the virus strain and patient factors. There is no specific cure treatment is mainly supportive, focusing on hydration, symptom management, and preventing complications. Since its identification in 1976, it has been responsible for 38 documented epidemics [2]. Utilizing fractional-order derivatives for mathematical modeling of biological events or other fields of science, has improved, during the recent decades. For example, a study presents a fractional-order SIR epidemic model with media and vaccination. It analyzes stability, identifies a threshold at $\mathcal{R}_0 = 1$, and formulates an optimal control strategy to minimize disease impact, supported by numerical simulations [3]. Raizah et al. study simulates Omicron variant spread using a fractional-order model solved via the Haar wavelet collocation method. The approach efficiently incorporates transmission factors to provide accurate dynamics insights [4]. The study of Li et al. develops a mathematical model to analyze monkeypox transmission between humans, animals, and the environment. A fractional-order version using the Caputo derivative is formulated to capture memory effects. The model's equilibria and stability are analyzed, parameters are fitted to 2022 US data, and numerical simulations illustrate the impact of memory and control measures on disease dynamics. [5] Mathematical modeling of Ebola virus disease (EVD) based on fractional calculus has demonstrated significant progress in recent years. This modeling approach enables researchers to develop effective strategies for understanding and controlling lethal infectious diseases, particularly Ebola. Below, we briefly summarize several recent studies investigating Ebola through fractional calculus frameworks. The study of Guedri et al., develops an Artificial Neural Network (ANN)-based framework to model EVD transmission and long-term disability outcomes. Extending an $SEIR$ model, it introduces a disability compartment to capture post-recovery chronic complications and incorporates delays to reflect the disease's natural progression more accurately [6]. Zhu et al., introduced a compartmental model for Ebola, incorporating transmission from deceased individuals and vaccination, to analyze dynamics and optimal control. Using data from Sierra Leone, they estimated the reproduction number and identifies effective time-dependent intervention [7]. Rhoubari et al., presented a generalized epizootic model for Ebola virus transmission in bats, incorporating environmental contamination. It used two flexible incidence functions to capture diverse transmission dynamics observed in infectious disease modeling [8]. Jafari et al., suggested an effective computational approach utilizing Bernstein's operational matrices and dual Bernstein polynomials to solve the nonlinear system of Ebola virus equations within the Caputo fractional framework [9]. Li et al., proposed a fractional-order Ebola model, analyzed its non-negative solutions, basic reproduction number, and equilibrium stabilities. To improve real-data accuracy, the Gorenflo-Mainardi-Moretti-Paradisi (GMMP) scheme solved the $SEIR$ system numerically, while modified grid approximation method (MGAM) estimated its parame-

ters [10]. Farman et al.'s study introduced a nonlinear fractional-order Ebola transmission model employing an innovative piecewise hybrid approach, structured across eight distinct compartments [11]. Zhang et al., investigated Ebola-malaria coinfections using a generalized Mittag-Leffler (M-L) kernel fractional derivative. Stability was assessed via Hyers-Ulam functional analysis, and a numerical scheme for the coinfection model was developed using Lagrange interpolation [12]. Ebola outbreaks occurred in communities with pet dogs that scavenged infected wildlife remains. Isaac K. Adu et al., developed a Caputo-Fabrizio derivative-based mathematical model to analyze Ebola transmission between dogs and humans. The research examined the model's solution existence and uniqueness using fixed-point theory [13].

In this article, we stratified the total human population into six distinct epidemiological compartments, susceptible, exposed, infectious, hospitalized, deceased but unburied, recovered, and denote these compartments with S, E, I, H, F and R, respectively. The main contribution of the authors is the development and rigorous analysis of a fractional-order Ebola model within the Caputo derivative framework, incorporating six compartments to explicitly account for hospitalization and post-mortem transmission, which are critical features of Ebola outbreaks. In essence, the authors provide both a theoretical foundation and a numerical tool for understanding and managing Ebola dynamics through the lens of fractional calculus, offering a more realistic representation of memory-dependent epidemic spread. In Section 1, we briefly describe the biological characteristics and transmission method of the EVD and mathematically review some academic studies conducted on this disease in recent years. In Section 2, we review the fundamental prerequisites and basic requirements necessary for studying this manuscript. The content of this section is primarily based on fractional calculus and mathematical biology. In Section 3, we introduce a fractional model in the Caputo sense for the EVD, which comprises six compartments or populations. By a diagram, we illustrate the transitions between all populations and derive the corresponding system of fractional differential equations. In Section 4, we determine the equilibrium points and the basic reproduction number for the Ebola model and prove that if the basic reproduction number equals 1, then a sharp threshold exists. This means the endemic equilibrium (EE) point exists only when the basic reproduction number is greater than 1, whereas the disease-free equilibrium (DFE) point always exists. In Section 5, we investigate the locally asymptotic stability (LAS) of the DFE point by applying the Routh-Hurwitz (R-H) criterion in the context of the Caputo derivative. The DFE is LAS when the basic reproduction number is less than 1. In Section 6, by defining appropriate Lyapunov functions, we examine the globally asymptotic stability (GAS) of the equilibrium points. This section also confirms the establishment of GAS with a sharp threshold for the basic reproduction number. In Section 7, by defining and introducing sensitivity indices, we analyze the sensitivity of the basic reproduction number to key parameters. The sensitivity analysis shows how changes in the magnitude of which parameters significantly affect the extent of the Ebola outbreak. In Section 8, using the generalized hat functions method, which has been comprehensively introduced by the authors in [14], we solve the system of fractional equations numerically, while the graphs corresponding to all populations are plotting, for different values of the fractional derivative order, and analyze the graphs from both numerical and epidemiological perspectives. Finally, in Section 9, we will summarize the discussions presented in this manuscript and provide some useful suggestions for future work, hoping they will be beneficial for interested readers.

2. Fundamental prerequisites

Prior to introducing our fractional-order disease model, it is essential to briefly present key definitions and theorems from dynamical systems theory, fractional calculus, and mathematical biology. These fundamental concepts will be employed throughout our analytical framework.

Definition 1. ([15]) Let $g \in AC^m([a,b])$, where $m \in \mathbb{N}$, and $\ell \in (m-1, m)$ be a fractional order. The Caputo derivative of order ℓ is defined as:

$$ {}_a^C D_t^\ell g(t) := \frac{1}{\Gamma(m-\ell)} \int_a^t \frac{g^{(m)}(\varepsilon)}{(t-\varepsilon)^{\ell+1-m}} d\varepsilon, $$

where $g^{(m)}$ is the m-th classical derivative of g $AC^m([a,b])$ denotes the space of functions with m absolutely continuous derivatives. Note that if $\ell = m$ then ${}_a^C D_t^\ell g(t) = g^{(m)}(t)$.

Remark 1. It is straightforward to show that for any complex constant z, the Caputo derivative of z vanishes, means that ${}_a^C D_t^\ell z = 0$ for all $\ell > 0$.

Definition 2. ([15]) The one-parameter and two-parameters M-L functions are defined as

$$ E_{\ell_1}(t) := \sum_{k=0}^{\infty} \frac{t^k}{\Gamma(k\ell_1 + 1)}, \quad E_{\ell_1,\ell_2}(t) := \sum_{k=0}^{\infty} \frac{t^k}{\Gamma(k\ell_1 + \ell_2)}. $$

Lemma 1. *([16]) Assume that, $t \geq 0$ and $\kappa \in \mathbb{R}$. Moreover, suppose that E_{ℓ_1,ℓ_2} is the two-parameter M-L function, then we have*

$$ \mathcal{L}\left\{ t^{\ell_2 - 1} E_{\ell_1,\ell_2}\left(-\kappa t^{\ell_1}\right) \right\} = \frac{s^{\ell_1 - \ell_2}}{s^{\ell_1} + \kappa}, \quad (\Re(s) > |\kappa|^{\frac{1}{\ell_1}}), $$

in which, $\Re(s)$ indicates the real part of Laplace variable s.

Assumption 1. *Consider the Caputo-type fractional dynamical system:*

$$ \begin{cases} {}_0^C D_t^\ell X = \mathbf{f}(t, X), & t > 0, \\ X(0) = X_0, \end{cases} \tag{2.1} $$

where $0 < \ell \leq 1$ denotes the fractional order, $X_0 \in \mathbb{R}^n$ represents the initial condition, $\mathbf{f} : \mathbb{R}_+ \times \Omega \to \mathbb{R}^n$ is a vector field satisfying piecewise continuity in t and local Lipschitz continuity in X (uniformly in t) and $\Omega \subseteq \mathbb{R}^n_+$ is an open domain.

Definition 3. ([17]) The fractional system (2.1) admits an equilibrium point, represented by a constant $\bar{X}$ for which $\mathbf{f}(t, \bar{X}) = \mathbf{0}$ holds.

Biological systems are inherently dynamic. Models of these systems, such as epidemiology SIR models for disease spread and biochemical networks are typically described by sets of nonlinear differential equations. The first step in analyzing such a system is to find its equilibrium points where the system does not change. The critical question is, what happens if the system is slightly perturbed from this equilibrium? Does it return to equilibrium? Means, is it locally stable? Does it spiral away into oscillation or chaos? In other word, is it unstable? This question of local stability is paramount. A stable equilibrium in a disease model might represent pathogen eradication, while an unstable one could represent an outbreak. The LAS of an equilibrium point is determined entirely by the eigenvalues of the Jacobian matrix evaluated at that point. The eigenvalues are found by solving the characteristic equation, which is a polynomial equation. finding the roots of this polynomial analytically, becomes extremely difficult, if not impossible, for polynomials of degree 4 and higher. This is where the R-H criterion becomes necessary. The R-H criterion provide a necessary and sufficient condition for determining whether all the roots of a polynomial have negative real parts without actually calculating the roots. It is an algorithmic procedure that uses only the coefficients of the characteristic polynomial, and allows us to derive analytical conditions on the parameters that guarantee stability.

Theorem 1. *([18]) Let $P(\omega) = \omega^m + c_1\omega^{m-1} + \cdots + c_{m-1}\omega + c_m$ be a polynomial of degree $m \in \mathbb{Z}^+$, such that $c_1, \ldots, c_m$ are real numbers. Moreover, let that the so-called Hurwitz matrices are defined as follows:*

$$H_1 := [c_1], \; H_2 := \begin{bmatrix} c_1 & 1 \\ c_3 & c_2 \end{bmatrix}, \; H_3 := \begin{bmatrix} c_1 & 1 & 0 \\ c_3 & c_2 & c_1 \\ c_5 & c_4 & c_3 \end{bmatrix}, \ldots, \; H_m := \begin{bmatrix} c_1 & 1 & 0 & 0 & \ldots & 0 \\ c_3 & c_2 & c_1 & 1 & \ldots & 0 \\ c_5 & c_4 & c_3 & c_2 & \ldots & 0 \\ \vdots & \vdots & \vdots & \vdots & \ddots & \vdots \\ 0 & 0 & 0 & 0 & \ldots & c_m \end{bmatrix},$$

where if $\jmath > m$, then $c_\jmath = 0$. Therefore, the polynomial $P(\omega)$ has all its roots either negative or with negative real parts if and only if the following determinant condition holds.

$$|H_\imath| = \det(H_\imath) > 0, \quad \imath = 1, 2, \ldots, m.$$

Theorem 2. *([19, 20, 21, 22]) Consider the fractional-order dynamical system (2.1). Let $J \in \mathbb{C}^{m\times m}$ be the Jacobian matrix evaluated at an equilibrium point, with eigenvalues $\{\omega_\imath\}_{\imath=1}^m$. Then, the equilibrium is LAS if and only if*

$$\min_{1\le\imath\le m} |\arg(\omega_\imath)| > \ell\frac{\pi}{2},$$

where $\ell \in (0, 1]$ is the fractional order, and $\arg(\cdot)$ denotes the complex argument.

Definition 4. ([18]) Consider the following dynamical system, which is described by the next equation.

$$\frac{d}{dt}X = \mathbf{f}(X),$$

where $X \in \mathbb{R}^n$ and $\mathbf{f} : \mathbb{R}^n \to \mathbb{R}^n$ is a locally Lipschitz function. A Lyapunov function for this system is a scalar function $V : \mathbb{R}^n \to \mathbb{R}$ that satisfies the following conditions:

1. Positive definiteness. $V(X) > 0, \forall X \neq \mathbf{0}$, and $V(\mathbf{0}) = 0$.
2. Radially unbounded (for global stability): $V(X) \to \infty$ as $\|X\| \to \infty$.
3. Negative semi-definite time derivative: $\frac{dV}{dt}(X) = \nabla V(X) \cdot \mathbf{f}(X) \le 0, \forall X \neq \mathbf{0}$ (for asymptotic stability, $\frac{dV}{dt}(X) < 0$ is required). Moreover, in the contex of Caputo, it is necessary to have ${}^C_0D^\ell_t V(X) \le 0$.

Lemma 2. *([14]) Suppose that $\bar{\mathcal{G}}$ is an equilibrium for self-directed fractional system, $\zeta \ge 0$ and $\ell \in (0, 1]$. Moreover, suppose that $\mathcal{G}(\zeta) \in \mathbb{R}^+$ is a real-valued differentiable function with a domain in $\mathbb{R}^+$. Then, we have*

$${}^C_0D^\ell_t \left(\mathcal{G}(\zeta) - \bar{\mathcal{G}} - \bar{\mathcal{G}} \ln \frac{\mathcal{G}(\zeta)}{\bar{\mathcal{G}}} \right) \le \left(1 - \frac{\bar{\mathcal{G}}}{\mathcal{G}(\zeta)} \right) {}^C_0D^\ell_t \mathcal{G}(\zeta),$$

Definition 5. ([18]) A set $\mathcal{PI} \subset \mathbb{R}^n$ is said to be positively invariant (PI) under a dynamical system, if for every initial condition $X_0 \in \mathcal{PI}$, the corresponding solution trajectory $X(t)$ remains contained in $\mathcal{PI}$ for all future time $t \ge 0$.

Remark 2. The PI property ensures permanent confinement of solutions within a specified region of state space. Lyapunov functions provide a constructive method for identifying invariant sets through their sublevel sets. This characterization is particularly useful for stability analysis of nonlinear systems.

The next theorem is known as LaSalle's invariance principle, and is used widely in case when global stability of an equilibrium point need to be examined.

Theorem 3. *([23]) Consider an autonomous system, $\frac{dX}{dt} = \mathbf{f}(X)$, where $\mathbf{f} : D \to \mathbb{R}^n$ is locally Lipschitz on a domain $D \subset \mathbb{R}^n$, and $\bar{X}$ is an equilibrium point. Let $V : D \to \mathbb{R}$ be a continuously differentiable positive definite function such that:*

$$\frac{dV(X)}{dt} = \nabla V(X) \cdot \mathbf{f}(X) \leq 0, \quad \forall X \in D.$$

If we define the set $S = \left\{ X \in D \mid \frac{dV(X)}{dt} = 0 \right\}$, and suppose that M be the largest invariant set contained in S, then every bounded trajectory of the system converges to M as $t \to \infty$.

Corollary 1. ([23]) If V is positive definite and $\frac{dV(X)}{dt}$ is negative semi-definite, and the only invariant subset of $S = \left\{ X \mid \frac{dV(X)}{dt} = 0 \right\}$ is $\{0\}$, then the origin is asymptotically stable.

The extension of LaSalle's invariance principle to fractional-order systems is a significant and active area of research. The core challenge is that the traditional proof and interpretation of LaSalle's principle rely heavily on the properties of integer-order derivatives and the structure of ODEs, which do not directly translate to the fractional calculus context. While a direct, one-to-one generalization of LaSalle's invariance principle for all fractional-order systems and all Lyapunov functions remains a topic of research, several powerful and practical extensions exist. The approach using the Caputo derivative with quadratic Lyapunov functions is the most well-established and widely used in the engineering literature, providing a robust tool for analyzing the asymptotic stability of a broad class of fractional-order systems.

Theorem 4. *([24]) Consider the fractional-order system with Caputo derivative:*

$${}_0^C D_t^\ell X(t) = \mathbf{f}(X),$$

where $\ell \in (0, 1), X \in \mathbb{R}^n$, $\mathbf{f}(\mathbf{0}) = \mathbf{0}$, and ${}_0^C D_t^\ell$ denotes the Caputo fractional derivative. Moreover, assume there exists a continuously differentiable Lyapunov function $V(X)$ such that:

1. *$V(X)$ is positive definite*
2. *${}_0^C D_t^\ell V(X) \leq 0$, for all $X \in D \setminus \{\mathbf{0}\}$, where D is a domain containing the origin.*
3. *The system trajectories $X(t)$ are bounded.*

Then, all trajectories converge to the largest invariant set contained in:

$$\mathcal{S} = \left\{ X \in D : {}_0^C D_t^\ell V(X) = 0 \right\}.$$

3. Constructing a model for Ebola disease transition

3.1. Constructing the Ebola model

We develop a fractional-order mathematical model in the sense of Caputo derivatives with order $\ell \in (0, 1]$ for EVD. As noted in the introduction, given the unique epidemiological characteristics of EVD where even deceased individuals can transmit the infection, we incorporate a compartment for deceased but unburied individuals denoted by F. Furthermore, we include a compartment for hospitalized cases, representing individuals

in the acute phase of illness requiring medical care and represent this compartment as H. The remaining compartments follow the conventional $SEIR$ framework. The use of mass-action incidence rate is justified for a theoretical fractional Ebola model focused on equilibrium stability, threshold behavior, and the impact of memory effects (ℓ). While more complex incidence forms could be adopted for detailed forecasting, the authors' choice aligns with the paper's primary aim, to establish a foundational fractional framework for Ebola dynamics that can later be extended with richer behavioral and contact structures. First and foremost, based on these considerations, we propose the following transmission model for EVD.

$$
\begin{aligned}
{}_0^C D_t^\ell S &= \Lambda - \beta S(I + \eta_H H + \eta_F F) - \mu S, && (3.1)\\
{}_0^C D_t^\ell E &= \beta S(I + \eta_H H + \eta_F F) - (\alpha + \mu)E, && (3.2)\\
{}_0^C D_t^\ell I &= \alpha E - (\gamma_H \theta + \gamma_I(1-\theta) + \gamma_D(1-\theta) + \mu)I, && (3.3)\\
{}_0^C D_t^\ell H &= \gamma_H \theta I - (\gamma_{DH} + \gamma_{RH} + \mu)H, && (3.4)\\
{}_0^C D_t^\ell F &= \gamma_D(1-\theta)I + \gamma_{DH} H - \gamma_F F, && (3.5)\\
{}_0^C D_t^\ell R &= \gamma_I(1-\theta)I + \gamma_{RH} H - \mu R. && (3.6)
\end{aligned}
$$

Second but not least, a diagram for the EVD transmission, is given in Figure 1. Beside this, all the parameters,

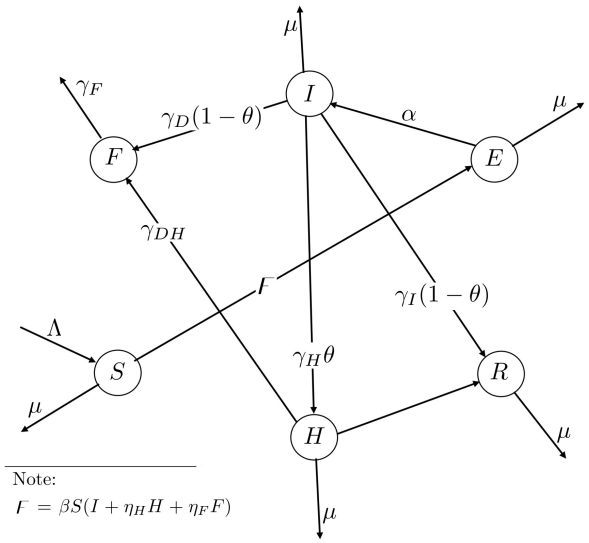


Fig. 1: Transmission of the proposed EVD model.

which are utilized in the EVD model described through the equations (3.1)-(3.6), with their corresponding measurement units and adequate explanations, have been listed in Table 1. Fractional-order models based on Caputo derivatives offer unique advantages that enable more accurate predictions of Ebola outbreaks compared to classical integer-order models. The fractional derivatives order $\ell \in (0, 1)$, in the Caputo model incorporate historical effects and long-range temporal dependencies in disease transmission [25, 26]. This feature is crucial for Ebola, whose outbreak patterns are influenced by varying environmental and behavioral factors over time [9]. In the study of EVD model, which is introduced through the equations (3.1)-(3.6), the following points are

noteworthy, as they enhance our understanding of the proposed EVD model. The force of infection includes transmission from infectious individuals, I, hospitalized patients, H, and unburied dead bodies, F. The model accounts for two routes of disease-induced mortality from I and H compartments. The burial rate, γ_F, reflects the importance of safe burial practices in Ebola control and the relative transmissibility parameters, η_H and η_F, account for different transmission risks. Equation (3.1) shows that susceptible individuals are recruited at rate Λ, can become infected through contact with infectious cases, hospitalized cases, or dead bodies, and experience natural mortality at rate μ. Equation (3.2) indicates that susceptible individuals become exposed at rate β, when they contact infectious individuals, with modified rates for contact with hospitalized patients, η_H, and dead bodies, η_F. Exposed individuals either progress to the infectious stage at rate α or die naturally at rate μ. The equation (3.3) shows that exposed individuals become infectious at rate α, after which they may be hospitalized proportion θ, at rate γ_H, recover without hospitalization proportion $1-\theta$, at rate γ_I, die from the disease without hospitalization proportion $1-\theta$, at rate γ_D, or experience natural mortality at rate μ. The fourth equation, (3.4), models infectious individuals who become hospitalized at rate $\gamma_H\theta$ and then either die from the disease at rate γ_{DH}, recover at rate γ_{RH}, or experience natural mortality at rate μ. The fifth equation, (3.5), tracks individuals who die from the disease either without hospitalization at rate $\gamma_D(1-\theta)$ or after hospitalization at rate γ_{DH}, and are then buried at rate γ_F. The final equation, (3.6), shows individuals who recover either without hospitalization at rate $\gamma_I(1-\theta)$ or after hospitalization at rate γ_{RH}, and then experience natural mortality at rate μ. Indeed, the use of Caputo fractional derivatives, rather than integer-order derivatives, allows the model to capture memory effects and long-range dependencies that may be significant in epidemic dynamics. This approach can better represent the complex patterns of disease spread, particularly for diseases like Ebola where transmission can occur through various routes and has shown complex temporal patterns.

Table 1: The model Parameters and their Description.

Parameter	**Description**	**Unit**
Λ	Recruitment rate of susceptible individuals	Day^{-1}
β	Transmission rate from infectious individuals	Day^{-1}
η_H	Relative transmissibility of hospitalized patients	Dimensionless
η_F	Relative transmissibility of unburied dead bodies	Dimensionless
μ	Natural mortality rate	Day^{-1}
α	Rate of progression from exposed to infectious	Day^{-1}
γ_H	Rate of hospitalization for infectious individuals	Day^{-1}
γ_I	Recovery rate for non-hospitalized individuals	Day^{-1}
γ_D	Disease-induced mortality rate	Day^{-1}
γ_F	Burial rate of dead bodies	Day^{-1}
γ_{DH}	Disease-induced mortality rate for hospitalized	Day^{-1}
γ_{RH}	Recovery rate for hospitalized individuals	Day^{-1}
θ	Proportion of infectious individuals hospitalized	Dimensionless

3.2. Positively invariant region

In this part, we are going to introduce a PI set for the solution of proposed Caputo fractional-order system that was described through the equations (3.1)-(3.6). The next lemma, Lemma 3, is an equivalent of the mean value theorem an will play a beneficial rule in our work.

Lemma 3. *Let $f(t) \in C[a,b]$, and moreover, postulate that for all $0 < \ell \leq 1$ the ${}_0^C D_t^\ell f(t)$ is existed on the interval $[a,b]$. Then, there exists a real value number like $\xi \in (a,t)$ such that*

$$\frac{1}{\Gamma(\ell+1)} \left({}_0^C D_t^\ell f\right)(\xi) = \frac{f(t)-f(a)}{(t-a)^\ell}, \quad \forall t \in (a,b],$$

and, moreover,

1. *If ${}_0^C D_t^\ell f(t) \geq 0$ for all $t \in (a,b]$, then $f(t)$ is non-decreasing on $[a,b]$.*
2. *If ${}_0^C D_t^\ell f(t) \leq 0$ for all $t \in (a,b]$, then $f(t)$ is non-increasing on $[a,b]$.*

Remark 3. For $\ell = 1$, since $\Gamma(2) = 1$ and ${}_0^C D_t^\ell f(t) = f'(t)$, Lemma 3 reduces exactly to the classical mean value theorem.

Theorem 5. *Consider the fractional-order dynamical system defined by (3.1)-(3.6), with initial conditions $S(0), E(0), I(0), H(0), F(0), R(0) > 0$, and all parameters $\Lambda, \beta, \mu, \alpha, \gamma_H, \gamma_I, \gamma_D, \gamma_{DH}, \gamma_{RH}, \gamma_F, \eta_H, \eta_F, \theta$ are positive constants, with $0 < \theta < 1$. Then, the solutions $S(t), E(t), I(t), H(t), F(t), R(t)$ remain positive for all time $t > 0$.*

Proof. We will now analyze each equation to show that, if a solution approaches to zero from above, its Caputo derivative cannot be negative, thus preventing it from becoming negative. Assume that, for the sake of contradiction, that there exists a first time $\mathcal{T}_1 > 0$ such that $S(\mathcal{T}_1) = 0$ and $S(t) > 0$ for $0 \leq t < \mathcal{T}_1$. At this point $\mathcal{T}_1$, if we evaluate the derivative, then we have:

$${}_0^C D_t^\ell S(\mathcal{T}_1) = \Lambda - \beta S(\mathcal{T}_1)\left(I(\mathcal{T}_1) + \eta_H H(\mathcal{T}_1) + \eta_F F(\mathcal{T}_1)\right) - \mu S(\mathcal{T}_1) = \Lambda - 0 = \Lambda > 0.$$

Since ${}_0^C D_t^\ell S(\mathcal{T}_1) > 0$, by utilizing the Lemma 3, $S(t)$ must be increasing at $\mathcal{T}_1$. This means that just before $\mathcal{T}_1$, $S(t)$ was less than zero to reach zero from above, but this contradicts our assumption that $S(t) > 0$ for $t < \mathcal{T}_1$. Therefore, our initial assumption is false, and $S(t)$ can never reach zero. Hence, $S(t) > 0$ for all $t > 0$. Now, given that we know S is always positive, we define the parameter $\mathcal{T}$ as

$$\mathcal{T} = \sup\{t \geq 0 : E(t), I(t), H(t), F(t) \text{ and } R(t) \geq 0\}.$$

Clearly, if $\mathcal{T} = +\infty$, then we conclude that E, I, H, F and $R(t)$ are all positive. Otherwise, suppose $\mathcal{T} < +\infty$, and the first function that changes sign from positive to negative at point $\mathcal{T}$ is E. This means there exists a positive real number ϵ such that E is negative on the interval $(\mathcal{T}, \mathcal{T}+\epsilon)$ and $E(\mathcal{T}) = 0$, while the other solutions of the proposed fractional system, (3.1)-(3.6), remain positive on this interval. Then, utilizing (3.2) lead us to the following.

$${}_0^C D_t^\ell E(\mathcal{T}) = \beta S(\mathcal{T})\left(I(\mathcal{T}) + \eta_H H(\mathcal{T}) + \eta_F F(\mathcal{T})\right) \geq 0.$$

Consequently, by applying Lemma 3, we conclude that E is increasing at point $\mathcal{T}$, which contradicts the assumption that E is negative on the interval $(\mathcal{T}, \mathcal{T}+\epsilon)$. Therefore, E never becomes negative for any $t > 0$. Regarding the other solutions of our fractional system, I, H, F and R, it can be easily proved, using a similar argument, that they also never become negative. Hence, by referring to the results proved above, we conclude that $\mathcal{T} = +\infty$, and the positivity of all solutions to the system of fractional equations expressed in relations (3.1)-(3.6) will be established. □

Theorem 6. *Let that $0 < \ell \leq 1$, and consider the fractional-order dynamical system, which is illustrated by (3.1)-(3.6), with positive initial conditions and parameters and $0 < \theta < 1$. Moreover, for clarity, the disease-induced death rate from the I compartment is written as $\gamma_D\delta(1-\theta)$ where δ is a fatality probability. Then, the solutions are uniformly bounded in forward time.*

Proof. First and foremost, we prove that the total living population, $N(t)$, is bounded, and for achieving this target, initially, we define the total living population, $N(t)$, as the sum of all individuals who are alive, means that we have the consequence.

$$N(t) = S(t) + E(t) + I(t) + H(t) + R(t).$$

Note that $F(t)$, fatalities, represents individuals who have died and are no longer in the living population. Lets find the Caputo derivative of $N(t)$. Using the linearity of the Caputo derivative:

$${}^{C}_{0}D^{\ell}_{t}N = {}^{C}_{0}D^{\ell}_{t}S + {}^{C}_{0}D^{\ell}_{t}E + {}^{C}_{0}D^{\ell}_{t}I + {}^{C}_{0}D^{\ell}_{t}H + {}^{C}_{0}D^{\ell}_{t}R.$$

Substituting the equations from the system that was described through the equations (3.1)-(3.6), approaches us to the followings.

$$\begin{aligned}
{}^{C}_{0}D^{\ell}_{t}N = &\Big(\Lambda - \beta S(I + \eta_H H + \eta_F F) - \mu S\Big) + \Big(\beta S(I + \eta_H H + \eta_F F) - (\alpha + \mu)E\Big) \\
&+ \Big(\alpha E - (\gamma_H\theta + \gamma_I(1-\theta) + \gamma_D\delta(1-\theta) + \mu)I\Big) + \Big(\gamma_H\theta I - (\gamma_{DH} + \gamma_{RH} + \mu)H\Big) \\
&+ \Big(\gamma_I(1-\theta)I + \gamma_{RH}H - \mu R\Big).
\end{aligned}$$

Now, we carefully add these terms, then we have the following.

$$\begin{aligned}
{}^{C}_{0}D^{\ell}_{t}N &= \Lambda - \mu S - \mu E - \mu I - \mu H - \mu R - \gamma_D\delta(1-\theta)I - \gamma_{DH}H + \gamma_{RH}H - \gamma_{RH}H \\
&= \Lambda - \mu(S + E + I + H + R) - \gamma_D\delta(1-\theta)I - \gamma_{DH}H.
\end{aligned}$$

Recognizing that $S + E + I + H + R = N$, and furthermore, $\gamma_D\delta(1-\theta)I \geq 0$ and $\gamma_{DH}H \geq 0$, approaches to thext consequence.

$${}^{C}_{0}D^{\ell}_{t}N \leq \Lambda - \mu N.$$

We can solve the previous using the comparison principle and properties of the M-L function. The solution of the inequality ${}^{C}_{0}D^{\ell}_{t}N(t) \leq \Lambda - \mu N(t)$, with initial condition $N(0) = N_0$, is bounded by the solution of the equation ${}^{C}_{0}D^{\ell}_{t}\widetilde{N}(t) = \Lambda - \mu\widetilde{N}(t)$, which is as follows.

$$\widetilde{N}(t) = N_0 E_\ell(-\mu t^\ell) + \Lambda \int_0^t (t-\tau)^{\ell-1} E_{\ell,\ell}(-\mu(t-\tau)^\ell)d\tau,$$

where E_ℓ and $E_{\ell,\ell}$ are M-L functions. A crucial property for boudedness is the asymptotic behavior, means $\lim_{t\to\infty}\widetilde{N}(t) = \frac{\Lambda}{\mu}$. This is the equilibrium of the fractional equation. Furthermore, for $0 < \ell \leq 1$, the M-L function $E_\ell(-\mu t^\ell)$ is completely monotonic and non-negative, ensuring the solution does not oscillate. Therefore, we can conclude that:

$$N(t) \leq \max\left(N(0), \frac{\Lambda}{\mu}\right), \quad \forall t \geq 0.$$

More precisely, for any $\epsilon > 0$, there exists a T such that for all $t > T$, $N(t) \leq \frac{\Lambda}{\mu} + \epsilon$. Thus, the total living population $N(t)$ is uniformly bounded in forward time.

Second and not least, for proving the boundedness of the fatalities compartment, $F(t)$, we examine the equation for the fatalities compartment F:

$$ {}_0^C D_t^\ell F = \gamma_D \delta (1-\theta) I + \gamma_{DH} H - \gamma_F F. $$

We know that $I(t)$ and $H(t)$ are bounded in advance, as they are part of the bounded total $N(t)$. Let M be an upper bound such that $I(t) \leq M$ and $H(t) \leq M$ for all $t \geq 0$. Then:

$$ \gamma_D \delta (1-\theta) I + \gamma_{DH} H \leq \gamma_D \delta (1-\theta) M + \gamma_{DH} M, $$

and if we define $\mathcal{K}$ as:

$$ \mathcal{K} := \gamma_D \delta (1-\theta) M + \gamma_{DH} M, $$

then $\mathcal{K}$ is a constant and $\gamma_D \delta (1-\theta) I + \gamma_{DH} H \leq \mathcal{K}$. So, we have the inequality:

$$ {}_0^C D_t^\ell F \leq \mathcal{K} - \gamma_F F. $$

This is of the same form as the inequality for $N(t)$. By the same reasoning, comparison principle, the solution $F(t)$ is bounded by the solution of ${}_0^C D_t^\ell \widetilde{F} = \mathcal{K} - \gamma_F \widetilde{F}$, which tends to $\frac{\mathcal{K}}{\gamma_F}$. Therefore, $F(t)$ is also uniformly bounded in forward time. □

Remark 4. Through the Theorems 5 and 6 , We have proven that, all compartment values are positive, and furthermore, all compartment values are bounded. Therefore, the solutions of the system are confined for all time $t > 0$ to a compact, positively invariant set $\Theta \subset \mathbb{R}_+^6$. We can explicitly define this set as next.

$$ \Theta = \left\{ (S, E, I, H, R, F) \in \mathbb{R}_+^6 : S + E + I + H + R \leq \frac{\Lambda}{\mu} + \epsilon_1 \text{ and } F \leq \frac{\mathcal{K}}{\gamma_F} + \epsilon_2 \right\} $$

where $\epsilon_1, \epsilon_2 > 0$ can be chosen arbitrarily small for the asymptotic result, or we can use the maximum values observed from the dynamics for a specific invariant set.

4. Equilibria and basic reproduction number

In mathematical models of disease spread, understanding a disease's long-term trajectory involves finding its equilibrium points. The most basic of these is the DFE. This is a stable scenario where the disease is entirely absent from the population, the counts of infected and exposed individuals are zero. The makeup of the population at this point is driven solely by demographic processes like birth, death, and sometimes vaccination, leaving only susceptible or recovered individuals. A key objective of public health measures like vaccination is to ensure this DFE is both reachable and stable, steering the population toward a future free of the pathogen. The feasibility of achieving this disease-free state hinges on a key metric called the basic reproduction number or R naught, and denoted as $\mathcal{R}_0$ in this paper. This value measures the average number of secondary cases generated by one infected person in a fully susceptible population. The DFE's stability is directly governed by $\mathcal{R}_0$. If $\mathcal{R}_0 < 1$, the disease cannot sustain an outbreak and any small introduction of the pathogen will fizzle out, allowing the system to revert to the DFE. Conversely, if $\mathcal{R}_0 > 1$, an initial

outbreak will occur, and the population will not return to a disease-free condition. Under conditions where $\mathcal{R}_0 > 1$, the system instead gravitates toward a different stable point known as the EE. Here, the disease becomes a permanent, self-sustaining presence in the community, maintaining a consistent, positive level of infection. This happens because the flow of individuals becoming infected and recovering is perfectly balanced by the birth of new susceptible and the loss of immunity. Unlike the DFE, the endemic state involves a constant mixture of susceptible, infected, and recovered individuals, representing a reality where the pathogen is permanently established. Analyzing this equilibrium allows health planners to gauge a disease's long-term impact and design continuous management strategies.

Theorem 7. *For the model described in (3.1)-(3.6), the DFE always exists.*

Proof. For the Ebola model with compartments S, E, I, H, F, R, the DFE is found by setting all infected compartments to zero. This means that the conditions $E = I = H = F = 0$ are satisfied, and by applying these conditions, the remaining equations concerning to the proposed EVD model, the equations (3.1)-(3.6), are simplified to the next.

$$
\begin{aligned}
&{}_0^C D_t^\ell S = \Lambda - \mu S,\\
&{}_0^C D_t^\ell R = -\mu R.
\end{aligned}
$$

This implies that

$$
X^0 := (S^0, E^0, I^0, H^0, F^0, R^0) = \left(\frac{\Lambda}{\mu}, 0, 0, 0, 0, 0\right),
$$

which indicates that, DFE always exists. □

Theorem 8. *For the model that is described in (3.1)-(3.6), the EE exists if and only if $\mathcal{R}_0 > 1$, which $\mathcal{R}_0$ is called the basic reproduction number.*

Proof. For the Ebola model with compartments S, E, I, H, F, R, we seek non-trivial solutions where the disease persists. If EE is denoted as $X^* := (S^*, E^*, I^*, H^*, F^*, R^*)$, all the time derivatives must be zero, at equilibrium.

$$
\begin{aligned}
&\Lambda - \beta S^*(I^* + \eta_H H^* + \eta_F F^*) - \mu S^* = 0,\\
&\beta S^*(I^* + \eta_H H^* + \eta_F F^*) - (\alpha + \mu)E^* = 0, &(4.1)\\
&\alpha E^* - \psi_1 I^* = 0, &(4.2)\\
&\gamma_H \theta I^* - \psi_2 H^* = 0, &(4.3)\\
&\gamma_D(1-\theta)I^* + \gamma_{DH} H^* - \gamma_F F^* = 0, &(4.4)\\
&\gamma_I(1-\theta)I^* + \gamma_{RH} H^* - \mu R^* = 0.
\end{aligned}
$$

Where $\psi_1 = \gamma_H\theta + \gamma_I(1-\theta) + \gamma_D(1-\theta) + \mu$ and $\psi_2 = \gamma_{DH} + \gamma_{RH} + \mu$. First, we express all variables in terms of I^*. From (4.2) we have

$$
E^* = \frac{\psi_1}{\alpha} I^*, \tag{4.5}
$$

from (4.3) we have

$$H^* = \frac{\gamma_H \theta}{\psi_2} I^*, \tag{4.6}$$

and from (4.4) we get the following

$$F^* = \frac{1}{\gamma_F}\left(\gamma_D(1-\theta)I^* + \gamma_{DH}H^*\right) = \frac{1}{\gamma_F}\left(\gamma_D(1-\theta) + \frac{\gamma_{DH}\gamma_H\theta}{\psi_2}\right) I^*. \tag{4.7}$$

If the force of infection is defined as $\lambda := \beta(I^* + \eta_H H^* + \eta_F F^*)$, and (4.6) and (4.7) are substituted, the following equation will be satisfied.

$$\lambda = \beta\left(1 + \eta_H\frac{\gamma_H\theta}{\psi_2} + \frac{\eta_F}{\gamma_F}\left(\gamma_D(1-\theta) + \frac{\gamma_{DH}\gamma_H\theta}{\psi_2}\right)\right) I^*.$$

And similarly, if we define

$$\Delta := 1 + \eta_H\frac{\gamma_H\theta}{\psi_2} + \eta_F\left(\frac{\gamma_D(1-\theta)}{\gamma_F} + \frac{\gamma_{DH}\gamma_H\theta}{\gamma_F\psi_2}\right), \tag{4.8}$$

then the next equation will be hold.

$$\lambda = \beta\Delta I^*. \tag{4.9}$$

Now, from (4.1) and (4.5) we have $\lambda S^* = (\alpha+\mu)E^* = (\alpha+\mu)\frac{\psi_1}{\alpha}I^*$, and by using (4.9), we obtain the following

$$S^* = \frac{(\alpha+\mu)\psi_1}{\alpha\beta\Delta}.$$

Furthermore, the total population $N = S + E + I + H + F + R$ satisfies the following.

$${}_0^C D_t^\ell N = \Lambda - \mu(N-F) - \gamma_F F = \Lambda - \mu N - (\gamma_F - \mu)F,$$

and at EE we have

$$N^* = \frac{1}{\mu}\left(\Lambda - (\gamma_F - \mu)F^*\right).$$

However, for simplicity we will proceed with the expression for S^*, and the foregoing discussion shows that

$$\begin{aligned}
&S^* = \frac{(\alpha+\mu)\psi_1}{\alpha\beta\Delta}, \quad E^* = \frac{\psi_1}{\alpha}I^*, \quad H^* = \frac{\gamma_H\theta}{\psi_2}I^*,\\
&F^* = \left(\frac{\gamma_D(1-\theta)}{\gamma_F} + \frac{\gamma_{DH}\gamma_H\theta}{\gamma_F\psi_2}\right)I^*, \quad R^* = \frac{\gamma_I(1-\theta)I^* + \gamma_{RH}H^*}{\mu},\\
&I^* = \frac{\Lambda - \mu S^*}{\beta\Delta S^*}.
\end{aligned} \tag{4.10}$$

Utilizing (4.10) leads to the following.

$$I^* = \frac{\mu}{\beta\Delta}\left(\frac{\Lambda\beta\Delta\alpha}{(\alpha+\mu)\mu\psi_1} - 1\right) = \frac{\mu}{\beta\Delta}(\mathcal{R}_0 - 1),$$

where $\mathcal{R}_0$ is the basic reproduction factor, and is defined as follows:

$$\mathcal{R}_0 := \frac{\alpha\beta\Lambda}{\mu(\alpha+\mu)\psi_1}\left(1 + \frac{\eta_H\gamma_H\theta}{\psi_2} + \frac{\eta_F\gamma_D(1-\theta)}{\gamma_F} + \frac{\eta_F\gamma_{DH}\gamma_H\theta}{\psi_2\gamma_F}\right).$$

Clearly, the EE exists when $I^* > 0$, which occurs when $\mathcal{R}_0 > 1$. □

5. LAS analysis of DFE in the fractional sense

The concept of LAS describes an equilibrium point that attracts nearby trajectories. Formally, it requires two properties. Stability, first, means that, trajectories starting sufficiently close remain arbitrarily close, and the other is attraction, these trajectories also converge to the equilibrium over time. In classical systems, a linear stability analysis shows that the equilibrium is LAS, as the eigenvalues of the corresponding Jacobian matrix all have negative real parts. This idea extends to fractional-order systems defined by Caputo derivatives. The LAS definition remains qualitatively the same, but the analysis differs. The stability criterion generalizes to $|\arg(\omega)| > \frac{\pi}{2}\ell$, where ℓ is the fractional order and ω is an arbitrary eigenvalue corresponding to the Jacobian matrix. Consequently, convergence is characterized by M-L functions, reflecting the memory and non-local properties of fractional calculus, rather than by exponential decay. As we know, the DFE is given by

$$X^0 = \left(\frac{\Lambda}{\mu}, 0, 0, 0, 0, 0\right),$$

where Λ is the recruitment rate of susceptible, and μ is the natural mortality rate. Now, applying the Theorem 1 for the case $n = 4$ leads to the following consequence that will be stated as next lemma.

Lemma 4. *With reference to Theorem 1, the R-H criterion for the case $n = 4$ and with characteristic polynomial of $J_{infected}$ (5.1) is given as follows:*

1. c_1, c_2, c_3 *and* $c_4 > 0$,
2. $c_1c_2c_3 > c_3^2 + c_1^2c_4$,
3. $c_1c_4 < c_2c_3$.

Theorem 9. *Concerning to the R-H criterion, the DFE is LAS if and only if, $\mathcal{R}_0 < 1$.*

Proof. The Jacobian matrix evaluated at X^0 is block-triangular:

$$J(X^0) = \begin{pmatrix} -\mu & 0 & -\beta S^0 & -\beta\eta_H S^0 & -\beta\eta_F S^0 & 0 \\ 0 & -(\alpha+\mu) & \beta S^0 & \beta\eta_H S^0 & \beta\eta_F S^0 & 0 \\ 0 & \alpha & -\psi_1 & 0 & 0 & 0 \\ 0 & 0 & \gamma_H\theta & -\psi_2 & 0 & 0 \\ 0 & 0 & \gamma_D(1-\theta) & \gamma_{DH} & -\gamma_F & 0 \\ 0 & 0 & \gamma_I(1-\theta) & \gamma_{RH} & 0 & -\mu \end{pmatrix}.$$

Focus on the infected subsystem (E, I, H, F):

$$J_{\text{infected}} = \begin{pmatrix} -(\alpha+\mu) & \beta S^0 & \beta\eta_H S^0 & \beta\eta_F S^0 \\ \alpha & -\psi_1 & 0 & 0 \\ 0 & \gamma_H\theta & -\psi_2 & 0 \\ 0 & \gamma_D(1-\theta) & \gamma_{DH} & -\gamma_F \end{pmatrix}.$$

The characteristic polynomial of J_{infected} is:

$$P(\omega) = \omega^4 + c_1\omega^3 + c_2\omega^2 + c_3\omega + c_4, \tag{5.1}$$

where, the coefficients are defined as:

$$c_1 = (\alpha+\mu) + \psi_1 + \psi_2 + \gamma_F, \tag{5.2}$$

$$c_2 = (\alpha+\mu)(\psi_1+\psi_2+\gamma_F) + \psi_1(\psi_2+\gamma_F) + \psi_2\gamma_F - \alpha\beta S^0, \tag{5.3}$$

$$c_3 = (\alpha+\mu)\psi_1\psi_2 + (\alpha+\mu)\psi_1\gamma_F + (\alpha+\mu)\psi_2\gamma_F + \psi_1\psi_2\gamma_F - \alpha\beta S^0\left(\psi_2 + \gamma_F + \gamma_H\theta\eta_H + \frac{\gamma_D(1-\theta)\eta_F}{\gamma_F}\right), \tag{5.4}$$

$$c_4 = (\alpha+\mu)\psi_1\psi_2\gamma_F(1-\mathcal{R}_0). \tag{5.5}$$

The R-H criterion for the case $n = 4$, is formulated according to the Lemma 4, and then we prove it step by step as the following. First of all, we prove that $c_1 > 0, c_2 > 0, c_3 > 0$ and $c_4 > 0$. As we know, all parameters, $\alpha, \mu, \gamma_F, \gamma_H, \gamma_I, \gamma_D, \gamma_{DH}, \gamma_{RH}$, are positive by definition. Thus from (5.2) clearly $c_1 > 0$. By (5.3), for c_2, the first three terms are sums of positive quantities:

$$(\alpha+\mu)(\psi_1+\psi_2+\gamma_F) > 0, \quad \psi_1(\psi_2+\gamma_F) > 0, \quad \psi_2\gamma_F > 0,$$

the subtracted term $\alpha\beta S^0$ is bounded by the stability condition $\mathcal{R}_0 < 1$. Substituting $\mathcal{R}_0 = \frac{\alpha\beta S^0\Delta}{(\alpha+\mu)\psi_1}$, where $\Delta > 0$, (see (4.8)), leads us to

$$\alpha\beta S^0 < \frac{(\alpha+\mu)\psi_1}{\Delta}.$$

Hence, the positive terms dominate, ensuring $c_2 > 0$. To prove the positivity of c_3, from (5.4) note that the first four terms are positive:

$$(\alpha+\mu)\psi_1\psi_2 > 0, \quad (\alpha+\mu)\psi_1\gamma_F > 0, \quad (\alpha+\mu)\psi_2\gamma_F > 0, \quad \psi_1\psi_2\gamma_F > 0.$$

The subtracted term

$$-\alpha\beta S^0\left(\psi_2 + \gamma_F + \gamma_H\theta\eta_H + \frac{\gamma_D(1-\theta)\eta_F}{\gamma_F}\right),$$

scales with $\mathcal{R}_0$. Since $\mathcal{R}_0 < 1$, the subtraction is outweighed by the positive terms, so $c_3 > 0$. Finally, for c_4, from (5.5) it is clear $c_4 > 0$ if and only if $\mathcal{R}_0 < 1$. Secondly, we need to prove that $c_1c_2c_3 > c_3^2 + c_1^2c_4$. As we mentioned before, all parameters $(\alpha, \mu, \gamma_F, \psi_1, \psi_2)$ are positive. Moreover, $a_1 > 0, a_2 > 0, a_3 > 0$ and $a_4 > 0$ when $\mathcal{R}_0 < 1$. The coefficient a_3 contains terms proportional to $\psi_1\psi_2, \psi_1\gamma_F, \psi_2\gamma_F$, minus smaller terms involving $\alpha\beta S^0$. Rewrite $c_1c_2c_3 > c_3^2 + c_1^2c_4$ as:

$$c_1c_2c_3 - c_3^2 > c_1^2c_4. \tag{5.6}$$

The left-hand-side (LHS) of (5.6) is

$$c_3(c_1c_2 - c_3) = \left(\text{Positive terms} - \text{Smaller terms proportional to } \alpha\beta S^0\right).$$

Applying(5.2), (5.3) and (5.4) and for $\mathcal{R}_0 < 1$, the positive terms dominate. So $c_1c_2 - c_3 > 0$. Furthermore, the right-hand-side (RHS) of (5.6) is

$$c_1^2c_4 = c_1^2(\alpha+\mu)\psi_1\psi_2\gamma_F(1-\mathcal{R}_0).$$

This grows quadratically but is scaled by $(1-\mathcal{R}_0) < 1$. Now, note that, $c_1c_2c_3$ grows cubically with ψ_1, ψ_2, γ_F. c_3^2 and $c_1^2c_4$ grow quadratically and for $\mathcal{R}_0 < 1$, the subtraction term $\alpha\beta S^0$ is reduced, preserving LHS dominance. So, we conclude that under the condition $\mathcal{R}_0 < 1$, the desired inequality obtained, which means that $c_1c_2c_3 > c_3^2 + c_1^2c_4$. Finally, we show that $c_1c_4 < c_2c_3$. To establish this inequality for the characteristic polynomial (5.1), we use the R-H stability criterion and the structure of the coefficients. Dividing both sides of $c_1c_2c_3 > c_3^2 + c_1^2c_4$ by c_1c_3, which are positive, by c_1c_3 leads to the next.

$$c_2 > \frac{c_3}{c_1} + \frac{c_1c_4}{c_3}.$$

This implies that $c_1c_4 < c_2c_3 - \frac{c_3^2}{c_1}$. From the positivity of coefficients, it follows that, $c_1c_4 < c_2c_3$. Finally, by utilizing R-H criteria we conclude that, the eigenvalues of J_{infected} have negative real parts if and only if $\mathcal{R}_0 < 1$. The remaining eigenvalues, from S and R, are $-\mu$, which are already negative. Hence, by Theorem 2, DFE is LAS and the desired results obtained. □

Remark 5. According to Theorem 2, the negativity of the real parts of the eigenvalues of the Jacobian matrix is a sufficient condition for the stability of the equilibrium point. However, this condition is not necessary when the disease follows a fractional epidemic model (see Theorem 2). In fact, for the DFE to be LAS in the Caputo sense, we must have $|\arg(\omega)| > \ell\frac{\pi}{2}$ where ω is any eigenvalue of the characteristic polynomial of the Jacobian matrix evaluated at DFE. Since we have proven that all roots of the characteristic polynomial are negative then we have $\arg(\omega) = -\pi$. Since $\ell \in (0, 1]$, then

$$|\arg(\omega)| = \pi > \frac{\pi}{2} > \ell\frac{\pi}{2},$$

which means that the condition $|\arg(\omega)| > \ell\frac{\pi}{2}$ is automatically satisfied.

6. GAS analysis of the equilibria

The concept of GAS is a fundamental and strong notion in the study of dynamical systems, crucial for understanding long-term behavior. In simple terms, an equilibrium point, a state where the system doesn't change, is GAS if it is globally attractive and LAS. Global attraction means no matter where we start the system in the entire state space, the system's trajectory will eventually approach this equilibrium point as time goes to infinity. The trajectories don't make wild jumps if we start near the equilibrium, we stay near it. This is often a consequence of the attraction property. This is a much stronger property than LAS, which only guarantees this behavior if the system starts sufficiently close to the equilibrium point. If an equilibrium is GAS, we know the system will inevitably settle there, regardless of initial disturbances or how far it was knocked away. It means the disease will eventually settle to a predictable state, like elimination or a constant endemic level, no matter how many initial infections there were. In summary, GAS is the gold standard for predictability in dynamical systems, ensuring that an equilibrium point is the inevitable final state for the entire system, no matter its starting point. A Lyapunov function can prove global stability, meaning the system will return to equilibrium from any starting point. It works directly with the nonlinear equations, capturing the full dynamics of the system, not just its linear approximation.

Theorem 10. *Assume that $\eta_H\gamma_F \geq \eta_F\gamma_{DH}$, then the DFE point is GAS if and only if $\mathcal{R}_0 < 1$.*

Proof. Firstly, note that the condition $\eta_H\gamma_F \geq \eta_F\gamma_{DH}$ is a mathematical encapsulation of a key Ebola control principle. The intervention impact on burial must outweigh the risk from corpses generated by hospital deaths. It aligns with WHO guidelines for Ebola, which states that, safe and dignified burial is as critical as hospital infection control, because transmission from corpses can be a major driver of outbreaks. The inequality ensures the model's stability analysis reflects this real-world intervention balance. Consider the Lyapunov function candidate as follows:

$$V_{\mathrm{DFE}} = E + \frac{\alpha+\mu}{\alpha} I + \frac{\beta\Lambda\eta_H}{\mu\psi_2} H + \frac{\beta\Lambda\eta_F}{\mu\gamma_F} F,$$

The Caputo derivative of V_{DFE} along trajectories of the system is:

$$\begin{aligned}
{}^{C}_{0}D^{\ell}_{t} V_{\mathrm{DFE}} &= {}^{C}_{0}D^{\ell}_{t} E + \frac{\alpha+\mu}{\alpha}\, {}^{C}_{0}D^{\ell}_{t} I + \frac{\beta\Lambda\eta_H}{\mu\psi_2}\, {}^{C}_{0}D^{\ell}_{t} H + \frac{\beta\Lambda\eta_F}{\mu\gamma_F}\, {}^{C}_{0}D^{\ell}_{t} F \\
&= \beta S(I + \eta_H H + \eta_F F) - (\alpha+\mu)E + \frac{\alpha+\mu}{\alpha}\left(\alpha E - \psi_1 I\right) + \frac{\beta\Lambda\eta_H}{\mu\psi_2}\left(\gamma_H\theta I - \psi_2 H\right) \\
&+ \frac{\beta\Lambda\eta_F}{\mu\gamma_F}\left(\gamma_D(1-\theta)I + \gamma_{DH} H - \gamma_F F\right).
\end{aligned}$$

At the DFE we have $S = \frac{\Lambda}{\mu}$, and then if $S \to S^0$ as $t \to \infty$, then we get the following

$$\begin{aligned}
{}^{C}_{0}D^{\ell}_{t} V_{\mathrm{DFE}} &= \beta\frac{\Lambda}{\mu}(I + \eta_H H + \eta_F F) - \frac{\alpha+\mu}{\alpha}\psi_1 I + \frac{\beta\Lambda\eta_H}{\mu\psi_2}(\gamma_H\theta I - \psi_2 H) \\
&+ \frac{\beta\Lambda\eta_F}{\mu\gamma_F}\left(\gamma_D\left(1-\theta\right) I + \gamma_{DH} H - \gamma_F F\right).
\end{aligned}$$

Simplifying the terms for I, H, and F yields the following relations:

$$\begin{aligned}
{}^{C}_{0}D^{\ell}_{t} V_{\mathrm{DFE}} &= I\left(\frac{\beta\Lambda}{\mu} + \frac{\beta\Lambda\eta_H\gamma_H\theta}{\mu\psi_2} + \frac{\beta\Lambda\eta_F\gamma_D(1-\theta)}{\mu\gamma_F} - \frac{\alpha+\mu}{\alpha}\psi_1\right) + H\left(\frac{\beta\Lambda\eta_F\gamma_{DH}}{\mu\gamma_F} - \frac{\beta\Lambda\eta_H}{\mu}\right) - \frac{\beta\Lambda\eta_F}{\mu}F \\
&= I\left(\frac{\beta\Lambda}{\mu}\left(1 + \eta_H\frac{\gamma_H\theta}{\psi_2} + \eta_F\frac{\gamma_D(1-\theta)}{\gamma_F}\right) - \frac{\alpha+\mu}{\alpha}\psi_1\right) + H\left(\frac{\beta\Lambda\eta_F\gamma_{DH}}{\mu\gamma_F} - \frac{\beta\Lambda\eta_H}{\mu}\right) - \frac{\beta\Lambda\eta_F}{\mu}F \\
&= I\left(\frac{(\alpha+\mu)\psi_1}{\alpha}\mathcal{R}_0 - \frac{\beta\Lambda\eta_F\gamma_{DH}\gamma_H\theta}{\mu\gamma_F\psi_2} - \frac{\alpha+\mu}{\alpha}\psi_1\right) + H\left(\frac{\beta\Lambda\eta_F\gamma_{DH}}{\mu\gamma_F} - \frac{\beta\Lambda\eta_H}{\mu}\right) - \frac{\beta\Lambda\eta_F}{\mu}F \\
&= I\left(\frac{(\alpha+\mu)\psi_1}{\alpha}(\mathcal{R}_0 - 1) - \frac{\beta\Lambda\eta_F\gamma_{DH}\gamma_H\theta}{\mu\gamma_F\psi_2}\right) + H\left(\frac{\beta\Lambda\eta_F\gamma_{DH}}{\mu\gamma_F} - \frac{\beta\Lambda\eta_H}{\mu}\right) - \frac{\beta\Lambda\eta_F}{\mu}F.
\end{aligned}$$

Since $H > 0$ and $\eta_H\gamma_F \geq \eta_F\gamma_{DH}$, then

$$H\left(\frac{\beta\Lambda\eta_F\gamma_{DH}}{\mu\gamma_F} - \frac{\beta\Lambda\eta_H}{\mu}\right) < 0,$$

and thus, for $\mathcal{R}_0 < 1$ we have

$${}^{C}_{0}D^{\ell}_{t} V_{\mathrm{DFE}} \leq -\frac{(\alpha+\mu)\psi_1}{\alpha}(1 - \mathcal{R}_0)I.$$

Since $\mathcal{R}_0 < 1$, then for all $I > 0$, the inequality ${}^{C}_{0}D^{\ell}_{t} V_{\mathrm{DFE}} < 0$ satisfies, which means that V_{DFE} is a Lyapunov function for DFE when $\mathcal{R}_0 < 1$ in the sense of Caputo and the desired result is obtained. □

REMARK 6. The condition $\eta_H\gamma_F \geq \eta_F\gamma_{DH}$, in fact, manages transmission from hospitalized individuals, η_H, and burial-related transmission, $\eta_F, \gamma_{DH}, \gamma_F$.

Theorem 11. *For the fractional model described in (3.1)-(3.6), if $\mathcal{R}_0 > 1$, the EE point is GAS, in the sense of Lyapunov.*

Proof. All in all, since the infectious compartments are E, I, H and F, we will define a function based on the deviations of these compartments from their EE values, and investigate it as a Lyapunov function candidate. A common and effective approach for epidemic models is to use a Volterra-type Lyapunov function. A suitable candidate Lyapunov function, L_{EE}, for the EE is a quadratic-like function of the form:

$$V_{EE} = \left(E - E^* - E^* \ln \frac{E}{E^*}\right) + A\left(I - I^* - I^* \ln \frac{I}{I^*}\right) + B\left(H - H^* - H^* \ln \frac{H}{H^*}\right) + C\left(F - F^* - F^* \ln \frac{F}{F^*}\right),$$

where $A, B, C > 0$ are positive constants to be determined. This function has the crucial properties as follows:

1. $V_{EE}(E^*, I^*, H^*, F^*) = 0$,
2. $V_{EE}(E, I, H, F) > 0$ for all $E, I, H, F > 0$ and $(E, I, H, F) \neq (E^*, I^*, H^*, F^*)$.

To prove stability for the Caputo fractional-order system, we need to show that the fractional derivative of L_{EE} along the trajectories of the system is negative semi-definite. Thus, applying lemma 2 results the next.

$$\begin{aligned}
{}^C_0D^\ell_t V_{EE} &\leq \left(1 - \frac{E^*}{E}\right) {}^C_0D^\ell_t E + A\left(1 - \frac{I^*}{I}\right) {}^C_0D^\ell_t I + B\left(1 - \frac{H^*}{H}\right) {}^C_0D^\ell_t H + C\left(1 - \frac{F^*}{F}\right) {}^C_0D^\ell_t F \\
&= \left(1 - \frac{E^*}{E}\right)(\beta S(I + \eta_H H + \eta_F F) - (\alpha + \mu)E) + A\left(1 - \frac{I^*}{I}\right)(\alpha E - \psi_1 I) \\
&+ B\left(1 - \frac{H^*}{H}\right)(\gamma_H \theta I - \psi_2 H) + C\left(1 - \frac{F^*}{F}\right)(\gamma_D(1-\theta)I + \gamma_{DH}H - \gamma_F F).
\end{aligned}$$

At the EE, the derivatives are zero. This gives us the following conditions.

1. $\beta S^*(I^* + \eta_H H^* + \eta_F F^*) = (\alpha + \mu)E^*$,
2. $\alpha E^* = \psi_1 I^*$,
3. $\gamma_H \theta I^* = \psi_2 H^*$,
4. $\gamma_D(1-\theta)I^* + \gamma_{DH}H^* = \gamma_F F^*$.

We can use these to simplify the expression for ${}^C_0D^\ell_t V_{EE}$. The goal is to group terms and choose constants A, B, C cleverly to make the derivative negative semi-definite. A standard choice is to select $A, B,$ and C such that the cross-terms involving E, I, H, F cancel out. From equilibrium condition 2, to balance the E^* and I^* terms, we can set $A = \frac{E^*}{I^*}$. Moreover, from equilibrium condition 3, to balance the I^* and H^* terms, we can set, $B = \frac{A\gamma_H\theta}{\psi_2} = \frac{E^*\gamma_H\theta}{I^*\psi_2}$, and eventually, in the same way, we set $C = \frac{A\eta_F\beta S^*}{\gamma_F} = \frac{E^*\eta_F\beta S^*}{I^*\gamma_F}$, to balance terms from the F^* equation. After substituting $A, B,$ and C and the equilibrium conditions, the expression for ${}^C_0D^\ell_t V_{EE}$ can be manipulated into a form that looks like the next.

$${}^C_0D^\ell_t V_{EE} \leq -\mu\frac{(S - S^*)^2}{S} + \beta S^*(I^* + \eta_H H^* + \eta_F F^*)\Xi\left(\frac{S}{S^*}, \frac{E}{E^*}, \frac{I}{I^*}, \frac{H}{H^*}, \frac{F}{F^*}\right).$$

Where $\Xi(\cdot)$ is a function that is non-positive by the arithmetic mean-geometric mean (AM-GM) inequality, i.e., $\Xi(\cdot) \leq 0$. By employing an approach analogous to what had been utilized by the authors in the proof of

Theorem 14 of [14], the explicit form of the function Ξ can be derived, and it can be readily established that $G \leq 0$. If we can show that ${}^{C}_{0}D^{\ell}_{t}V_{EE} \leq 0$ for all states and ${}^{C}_{0}D^{\ell}_{t}V_{EE} = 0$ only at the equilibrium, then by the fractional Lyapunov stability method, the EE is GAS. The positivity of parameters A, B, and C ensures that the I^* component of the EE is also positive. Consequently, by applying Theorem 8, this implies $\mathcal{R}_0 > 1$. It follows that the function V_{EE} serves as a Lyapunov function at the EE, or equivalently, the EE is GAS if and only if $\mathcal{R}_0 > 1$. □

7. Sensitivity analysis

In epidemic modeling, a sensitivity index measures how much a model's output changes in response to a small change in one of its input parameters. It quantifies the sensitivity or responsiveness of the model to each parameter Consider that an epidemic model is a complex machine with many dials, parameters like transmission rate, recovery rate and so on. The sensitivity index tells us which dials, when turned just a little, have the biggest impact on the machine's final output, means the total number of infected people, the peak of the epidemic, or the basic reproduction number. The most common way to calculate this is using the normalized forward sensitivity index, which is a dimensionless measure. For a parameter ϑ and an output of interest $\mathcal{Y}$ (like $\mathcal{R}_0$), the sensitivity index, $\Upsilon^{\mathcal{Y}}_{\vartheta}$, is defined as [14, 27, 28]:

$$\Upsilon^{\mathcal{Y}}_{\vartheta} = \frac{\vartheta}{\mathcal{Y}} \times \frac{\partial \mathcal{Y}}{\partial \vartheta}.$$

This formula essentially calculates the percentage change in the output $\mathcal{Y}$ resulting from a 1 percent change in the input parameter ϑ. If $\Upsilon^{\mathcal{Y}}_{\vartheta} > 0$, the output $\mathcal{Y}$ increases as the parameter ϑ increases. They have a direct relationship. If $\Upsilon^{\mathcal{Y}}_{\vartheta} < 0$, the output $\mathcal{Y}$ decreases as the parameter ϑ increases. They have an inverse relationship. Moreover, $|\Upsilon^{\mathcal{Y}}_{\vartheta}|$ indicates the strength of the influence. Sensitivity indices for the most effective parameters are illustrated in Table 2. According to the obtained result from Table 2 we can say that with an increase in the values of parameters $\mu, \gamma_F, \gamma_{RH}$ and γ_I, R naught decreases, consequently reducing the disease outbreak in the community. In other words, if the natural mortality rate, burial rate of dead bodies, recovery rate for hospitalized individuals and recovery rate for non-hospitalized individuals in the community increase, the rate of disease progression within the community decreases. On the other hand, a decrease in the values of parameters $\Lambda, \beta, \eta_H, \eta_F, \gamma_H$ and α tend to a decline in R naught, resulting in disease control within the community. This implies that by reducing the rate of population influx into the community, transmission rate from infectious individuals, relative transmissibility of hospitalized patients, relative transmissibility of unburied dead bodies, rate of hospitalization for infectious individuals and the rate of progression from exposed to infectious, the R naught will also decrease, consequently leading to the disease being controlled or, in an ideal scenario, eradicated from the community.

8. Numerical discussion using real-word data from Ebola outbreak in Africa 2014

In this part, the aim is to investigate and to examine all of the theoretical results attained throughout this study. First and foremost, we utilize the most applicable and popular generalized hat functions (GHFs) approach, which had been proposed by authors [14], and solve the fractional system (3.1)-(3.6), according to the quantities for the value of parameters where are listed in Table 3. Last but not least, we numerically investigate the behavior of our model that is described by (3.1)-(3.6). To properly evaluate the accuracy of the model introduced in this manuscript, it is preferable to use real-world data as the parameter values.

Table 2: Sensitivity indices corresponding to the most effective parameters with their signs.

Parameter	$\Upsilon^{\mathcal{R}_0}_{\text{Parameter}}$	Sign of $\Upsilon^{\mathcal{R}_0}_{\text{Parameter}}$	Effect on $\mathcal{R}_0$
μ	$-\mu\left(\frac{1}{\mu}+\frac{1}{\alpha+\mu}+(1-\theta)\frac{\gamma_I+\gamma_D}{\psi_1}\right)$	Negative	Decrease
γ_F	$-\frac{\eta_F}{\gamma_F\Delta}\left((1-\theta)\gamma_D+\theta\frac{\gamma_{DH}\gamma_H}{\psi_2}\right)$	Negative	Decrease
γ_{RH}	$-\frac{\gamma^2_{RH}}{\psi_2}$	Negative	Decrease
γ_I	$-\frac{\gamma^2_I(1-\theta)}{\psi_1\mathcal{R}_0}$	Negative	Decrease
Λ	$+1$	Positive	Increase
β	$+1$	Positive	Increase
η_H	$+\theta\frac{\eta_H\gamma_H}{\Delta\psi_2}$	Positive	Increase
η_F	$+\frac{\eta_F}{\Delta}\left((1-\theta)\frac{\gamma_D}{\gamma_F}+\theta\frac{\gamma_{DH}\gamma_H}{\gamma_F\psi_2}\right)$	Positive	Increase
γ_H	$+\theta\frac{\gamma_H}{\Delta\psi_2}\left(\eta_H+\eta_F\frac{\gamma_{DH}}{\gamma_F}\right)$	Positive	Increase
α	$+\frac{\mu}{\alpha+\mu}$	Positive	Increase

Although access to such real data posed a challenge for the authors, by examining several research studies ([29, 30, 31, 32]) related to the 2014 Ebola outbreak in West Africa, they were able to obtain values for the parameters used in the proposed Ebola model. This effort enables a more precise alignment of the model with an actual Ebola outbreak. The study [29] refers to populations affected by the Ebola virus disease during the 2014-2016 outbreak in West Africa, specifically in Guinea, Liberia, Sierra Leone, Nigeria, Mali, Senegal and Democratic Republic of Congo. The population data include total population of each country, number of reported cases, number of deaths, case fatality rates (CFR) and incidence proportion per 100,000 people. In research [30] The data were obtained from the WHO from 6 July to 9 August 2014 and Socioeconomic Data and Applications Center (SEDAC) at Columbia University. They collected data from over 80,000 administrative regions across 5 continents. In [31], the authors gathered related data that reported by WHO from December 2013 to 20 April 2014. Ultimately, with regard to research [32], dataset types include surveillance, clinical cohorts, genomic sequences, facility assessments, programmatic data, vaccine trials, and literature. Population include more than 28,000 EVD patients, more than 17,000 survivors, 200,000 HIV patients and approximately 7,500 vaccine volunteers. The most utilized literature sources in this research are peer-reviewed journals Lancet, NEJM, Science, J Infect Dis, PLoS NTDis, Emerg Infect Dis, Nat Med and J Clin Invest. So, suppose that the number of individuals in each compartment is normalized by a large number such as 10^5 individuals, and moreover, assume that the initial values for the compartment magnitude are adopted as $S_0 = 0.74, E_0 = 0.0001, I_0 = 0.0001, H_0 = 0.01, F_0 = 0.2, R_0 = 0.1$ [29]. We have obtained the equilibria as follows.

$$X^0 = [1.5741, 0, 0, 0, 0, 0]^T,$$
$$X^* = [0.5260, 0.6404, 0.2429, 0.1136, 0.5046, 0.0402]^T.$$

Note that, for the DFE case we have, $\mathcal{R}_0 = 0.1037 < 1$ and it is stable, while for the EE case we have, $\mathcal{R}_0 = 3.3447 > 1$, which is also stable. For both equilibrium states (DFE and EE), and applying various fractional derivative orders $\ell \in \{0.75,\ 0.8,\ 0.85\ , 0.9,\ 0.95,\ 1\}$, the corresponding diagrams are illustrated in Figures 2 and 3. Firstly, looking at the Figure 2, ones can find that, susceptible population $S(t)$, starts at the initial normalized value $S_0 = 0.74$, shows a gradual decline as individuals become exposed or infected. It eventually stabilizes at the DFE value $S^0 \approx 1.5741$, which is higher than the initial value because the model

Table 3: The value of parameters in order to the prposed Ebola model.

Parameters	DFE case	EE case	Source
Λ	0.85	0.95	Assumed
β	0.09	0.09	[29]
η_H	0.03	0.5	Assumed
η_F	0.8	0.8	Assumed
μ	0.54	0.54	[30]
α	0.5	0.5	Assumed
γ_H	0.67	0.67	[30]
γ_I	0.2	0.2	Assumed
γ_D	0.74	0.74	[29]
γ_F	0.21	0.21	[31]
γ_{DH}	0.3	0.3	[31]
γ_{RH}	0.02	0.02	Assumed
θ	0.6	0.6	[32]

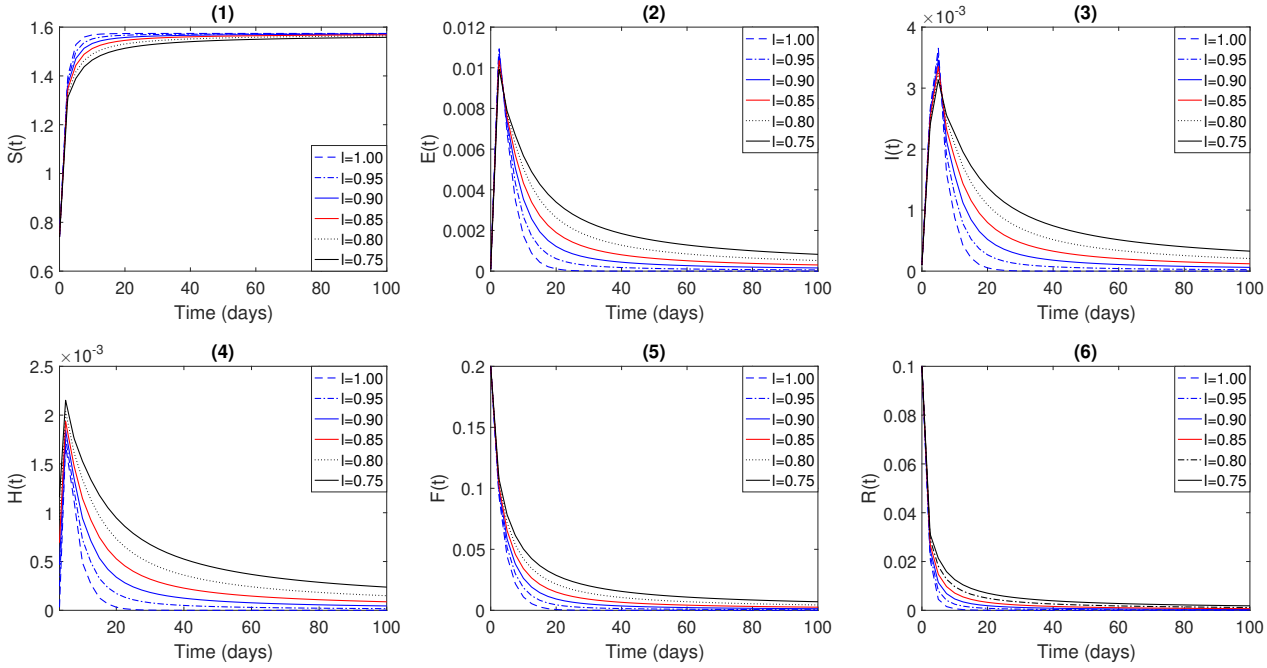


Fig. 2: The results of proposed Ebola model, when the DFE case happens.

accounts for recruitment Λ and natural mortality μ. Exposed population $E(t)$, begins at a very low initial value $E_0 = 0.0001$, exhibits a sharp peak early in the outbreak, reflecting rapid initial spread. The peak is higher and occurs later for smaller ℓ. After the peak, $E(t)$ declines to zero as the disease dies out. Infectious

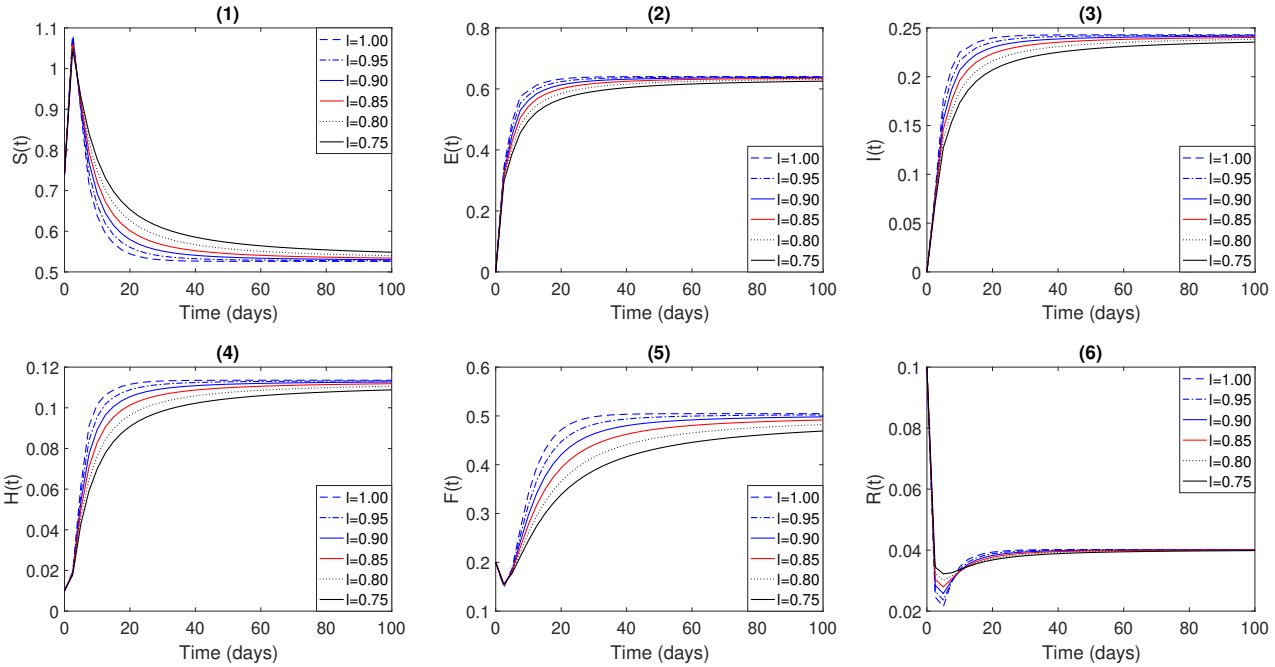


Fig. 3: The results of proposed Ebola model, when the EE case happens.

population $I(t)$, starts at $I_0 = 0.0001$. Also shows a sharp peak, slightly delayed compared to $E(t)$, as exposed individuals become infectious. The peak magnitude decreases with larger ℓ, and the decline to zero is slower for smaller ℓ. Hospitalized population $H(t)$, starts at $H_0 = 0.01$. It follows a similar sharp peak pattern as $I(t)$, but with lower magnitude due to the hospitalization proportion θ, returns to zero as the outbreak ends. Deceased but unburied population $F(t)$, begins at $F_0 = 0.2$, demonstrates a sharp rise and fall, reflecting the accumulation of deaths during the peak infection period, followed by burials at rate γ_F, and eventually decays to zero in the DFE. Recovered population $R(t)$, starts at $R_0 = 0.1$, increases gradually during the outbreak as individuals recover. Then stabilizes as the outbreak ends. In DFE, $R(t)$ also tends to zero because of no immunity in the model beyond recovery, and recovered individuals eventually die naturally. Now let us focus on the three sharp peaks. Peak in $E(t)$ represents the maximum number of individuals in the latent phase, occurs early in the outbreak, indicating rapid initial transmission. The peak is higher and later for smaller ℓ, showing that fractional memory effects prolong the buildup of exposed cases. Peak in $I(t)$ follows shortly after the peak in $E(t)$, as exposed individuals become infectious, and reflects the height of the active outbreak. Smaller ℓ leads to broader, delayed peaks, suggesting a slower progression to and from the infectious stage. Peak in $H(t)$ after $I(t)$, as deaths accumulate from the infectious and hospitalized compartments, demonstrates the lethality of Ebola and the role of hospitalized practices in transmission. Again, smaller ℓ results in a later, more drawn-out mortality curve. All peaks diminish and eventually vanish as $t \to \infty$, confirming that the DFE is reached when $\mathcal{R}_0 < 1$. Fractional order ℓ influences timing and sharpness. Lower ℓ tends to slower dynamics, later peaks, longer outbreak duration. Higher ℓ causes faster dynamics, earlier peaks, quicker convergence to DFE. The sharpness of peaks reflects the high transmissibility and rapid progression of Ebola, especially in

the early phase. The sequential ordering of peaks, $E \to I \to F$, aligns with the natural history of Ebola infection. Moreover, A detailed examination of sections (2), (3) and (4) of Figure 2 leads to the conclusion that the Ebola virus initially spreads at a very high rate. The sharp peaks in charts (2), (3) and (4) confirm this observation. As is known, the Ebola virus has a short incubation period, and an infected individual in this phase, if not promptly treated, becomes highly infectious at a rapid pace.

Secondly, Figure 3 presents the numerical simulation results for the proposed fractional Ebola model when the EE is reached. Susceptible population $S(t)$ starts at $S_0 = 0.74$. Then, declines sharply as the outbreak takes off, due to high transmission. It stabilizes at a lower endemic level $S^* \approx 0.5260$, indicating a persistent pool of susceptibles in the endemic state. Curve of $E(t)$ starts at $E_0 = 0.0001$, indicates a rapid, sharp peak early in the outbreak, similar to Figure 3. However, unlike in the DFE case, $E(t)$ does not drop to zero, it settles to an endemic equilibrium $E^* \approx 0.6404$, meaning the disease remains circulating in the population. Infectious compartment $I(t)$ starts at $I_0 = 0.0001$ and peaks sharply after $E(t)$, then declines but stabilizes at $I^* \approx 0.2429$. This non-zero steady state confirms the persistence of the disease in the community. Hospitalized population $H(t)$ begins at $H_0 = 0.01$ and follows the infectious curve, peaking and then sustaining at $H^* \approx 0.1136$. The endemic level reflects ongoing hospitalization needs in an endemic scenario. Deceased (unburied) individuals $F(t)$ start at $F_0 = 0.2$ and show a sharp rise during the outbreak peak, then stabilize at $F^* \approx 0.5046$. The non-zero equilibrium indicates ongoing mortality due to the disease in the endemic state. The curve od recovered population $R(t)$ starts at $R_0 = 0.1$. Then it increases and stabilizes at $R^* \approx 0.0402$, reflecting a steady proportion of recovered individuals in the endemic population. Figure 3 has three sharp points. Peak in $S(t)$, represents the rapid depletion of susceptibles during the explosive initial outbreak phase.The steepness is due to the high force of infection $\lambda = \beta(I+\eta_H H+\eta_F F)$, which is large because I, H, F grow quickly. The curve is steeper for higher ℓ closer to 1, meaning classical models predict a faster initial burn-through of susceptibles. The decline flattens as the system approaches the endemic equilibrium, where the recruitment of new susceptibles balances new infections. The sharp drop in $S(t)$ signifies the loss of herd immunity and the uncontrolled spread in the early phase. Rapid rise $F(t)$ increases sharply as deaths accumulate from the infectious and hospitalized compartments. This rise lags behind $I(t)$ because death follows infection. The peak occurs when the rate of new deaths equals the burial rate ($\gamma_F F$). After this point, burials outpace new deaths. Eventually, in $R(t)$ individuals, few are recovering because the infectious pool is small. As $I(t)$ and $H(t)$ peak, the recovery streams $\gamma_I(1-\theta)I$ and $\gamma_{RH}H$ surge, causing $R(t)$ to increase at its maximum rate. This is the steep, almost linear mid-section of the curve. Moreover, it is mentionable that, if we consider parts (2) and (4) of Figure 3, it can be observed that graphs of exposed individuals, $E(t)$ and the hospitalized persons' compartment, $H(t)$, reach equilibria more rapidly than the other sections of Figure 3. It should be noted, however, that the rapid attainment of EE for graph $E(t)$ indicates that the latent period for Ebola in the endemic state is short, and individuals in the community become infectious shortly after contracting the Ebola virus. Furthermore, the rapid achievement of EE in section related to $H(t)$ underscores the effectiveness of hospital care in controlling the disease. Although it is known that fractional derivatives, particularly the Caputo derivative, represent the inherent nature of natural phenomena, especially epidemics, more accurately and realistically, ensuring that a specific epidemic follows a fractional model with a particular Caputo derivative order requires precise case-specific and clinical studies within the affected population. Only after conducting such detailed studies can the results from clinical investigations be evaluated using the model and method introduced and investigated in this study.

9. Summary and conclusion

In this manuscript, we presented a comprehensive fractional-order epidemic model for EVD using the Caputo derivative framework. The model divided the population into six compartments, susceptible, exposed, infectious, hospitalized, deceased, and recovered. We proved the validity and positivity of the fractional system's solutions. Moreover, we introduced a PI set for the solution space. The numerical simulations revealed that the fractional order ℓ acts as a temporal scaling parameter that modulates the speed and trajectory of the Ebola outbreak without altering the final endemic or disease-free equilibrium states. Specifically, when ℓ is reduced from 1, the classical integer-order case, to lower values such as 0.75, the epidemic peak is delayed, the ascent and the descent phases are prolonged, and convergence to equilibrium slows significantly. This demonstrated that memory effects captured by the fractional derivative produce more realistic, protracted outbreak dynamics consistent with observed Ebola patterns, where behavioral adaptation, intervention delays, and healthcare system inertia stretch the epidemic timeline. Importantly, while ℓ influences the transient dynamics, it does not change the threshold condition $\mathcal{R}_0 = 1$ or the stability of equilibria, underscoring that fractional modeling enriches the temporal representation of outbreak progression while preserving the fundamental regulatory role of the basic reproduction number. Formulation of a fractional $SEIHFR$ model that accounts for post-mortem transmission and hospitalization, derivation of the basic reproduction number, $\mathcal{R}_0$, and analysis of DFE and EE points, are the key contributions. Moreover, the stability analysis using R-H criterion for LAS of DFE, and Lyapunov function for GAS of both DFE and EE were the other aspects of our contributions. Sensitivity analysis is applied to identify parameters most influencing $\mathcal{R}_0$. Numerical simulations using generalized hat functions were utilized to solve the fractional system, illustrating the impact of the fractional order ℓ on disease dynamics. The study demonstrated that the DFE is stable when $\mathcal{R}_0 < 1$, and the EE is stable when $\mathcal{R}_0 > 1$, the fractional order ℓ significantly affects the convergence speed of solutions such that, values closer to 1 lead to faster convergence to equilibrium. Furthermore, key parameters such as transmission rate, β, burial rate, γ_F, and hospitalization rate, θ, critically influenced, $\mathcal{R}_0$, and outbreak control. Beside these, the Caputo fractional model effectively captured memory effects and long-range dependencies, were offering a more realistic representation of Ebola dynamics compared to classical integer-order models. This model provides valuable theoretical and numerical insights for public health strategies, including hospitalization, safe burial practices, and contact reduction, to control and prevent Ebola outbreaks. It should be noted that although the authors have presented the model depicted in Figure 1 for Ebola disease transmission, it is important to recognize that this model can be highly flexible. By introducing modifications, different models for Ebola can be derived, each capable of analyzing the disease from perspectives different from those explored in this article. As a suggestion for future work, adding components such as vaccination or quarantine compartments, changing the transmission rate, for instance, by using a standard or saturated incidence rate, removing the exposed compartment under the assumption of a short latent period, which allowing direct transition from the susceptible to the infectious compartment, or employing other fractional derivatives and operators instead of the Caputo fractional derivative, can lead to various distinct models. Each of these models can study the Ebola disease from a specific and unique standpoint, and undoubtedly, they would have the specific features that will be of interest.

Data Availability Statement

All data generated or analysed during this study are included in this published article.

Conflict of Interest

The authors declare no conflicts of interest.

Funding Information

There is no funding associated with this article.

Author Contribution

S. Kosari was responsible for conceptualization, methodology development, software implementation, validation, and drafting the original manuscript. **M. H. Heydari** participated in conceptualization, methodology design, software implementation, and validation, while also handling manuscript review and editing, and visualization, and supervision. **D. Baleanu** contributed to conceptualization, methodology design, software implementation, and validation, while also handling manuscript review and editing, and visualization. **M. Bayram** contributed to conceptualization, methodology design, software implementation, and validation, while also handling manuscript review and editing, and visualization.

References

[1] P. Yadav, S. Jahan, and K.S. Nisar. Fractional order mathematical model of Ebola virus under Atangana-Baleanu-Caputo operator. *Results in Control and Optimization*, 13:100332, 2023.

[2] R. K. Nash, S. Bhatia, C. Morgenstern, P. Doohan, D. Jorgensen, K. McCain, R. McCabe, D. Nikitin, G. C. Dannenburg, J.T. Hicks, et al. Ebola virus disease mathematical models and epidemiological parameters: A systematic review. *The Lancet Infectious Diseases*, 24(12):762–773, 2024.

[3] S. Barman, S. Jana, S. Majee, S. Patra, and T.K.Kar. Impact of vaccination and media on a Caputo derivative-based fractional-order epidemic model with PRCC analysis: S. Barman et al. *International Journal of Dynamics and Control*, 13(9):293, 2015.

[4] Z. Raizah, and R. Zarin. Advancing COVID-19 understanding: Simulating omicron variant spread using fractional-order models and haar wavelet collocation. *Mathematics*, 11(8):1925, 2023.

[5] C. Li, S. Ullah, R. Nawaz, S.A. Al-Qahtani, S. Li, and others. Mathematical modeling and analysis of monkeypox 2022 outbreak with the environment effects using a Cpauto fractional derivative. *Physica Scripta*, 98(10):105239, 2023.

[6] K. Guedri, R. Zarin, M. Oreijah, S.K. Alharbi, and H.A.W. Khalifa. Artificial neural network-driven modeling of Ebola transmission dynamics with delays and disability outcomes. *Computational Biology and Chemistry*, 15(6):1208, 2023.

[7] Q. Zhu, M. Asim, S. Ullah, A.A. Khan, and others. Nonlinear dynamical modeling and control of Ebola involving transmission from hospitalized and deceased populations: a data-driven approach from Sierra Leone. *Journal of Applied Mathematics and Computing*, 72(1):35, 2026.

[8] Z.E. Rhoubari, H. Besbassi, K. Hattaf, and N. Yousfi. Mathematical modeling of Ebola virus disease in bat population. *Discrete Dynamics in Nature and Society*, 2018(1):5104524, 2018.

[9] I. Masti, K. Sayevand, and H. Jafari. On epidemiological transition model of the Ebola virus in fractional sense. *J. Appl. Anal. Comput.*, 14(3):1625–1647, 2024.

[10] W. Pan, T. Li, and S. Ali. A fractional order epidemic model for the simulation of outbreaks of Ebola. *Advances in Difference Equations*, 2021:1–21, 2021.

[11] K.S. Nisar, M. Farman, K. Jamil, A. Akgul, and S. Jamil. Computational and stability analysis of Ebola virus epidemic model with piecewise hybrid fractional operator. *Plos one*, 19(4):0298620, 2024.

[12] L. Zhang, E. Addai, J.A. Prah, Y.D. Arthur, and J.K.K. Asamoah. Fractional-Order Ebola-Malaria Coinfection Model with a Focus on Detection and Treatment Rate. *Computational and Mathematical Methods in Medicine*, 2022(1):6502598, 2022.

[13] I.K. Adu, F.A. Wireko, E.N.O. Mojeeb Al-R, and J.K.K. Asamoah. A fractional order Ebola transmission model for dogs and humans. *Scientific African*, 24:02230, 2024.

[14] S. Kosari, M.H. Heydari, M. Razzaghi, and M. Bayram. Studying the stability of the cholera fractional model and its simulation using generalized hat basis functions. *Results in Physics*, 108369, 2025.

[15] I. Podlubny. *Fractional differential equations: An introduction to fractional derivatives, fractional differential equations, to methods of their solution and some of their applications*, volume 198. elsevier, 1998.

[16] L. Kexue, and P. Jigen. Laplace transform and fractional differential equations. *Applied Mathematics Letters*, 24(12):2019–2023, 2011.

[17] Y. Li, Y. Chen, and I. Podlubny. Stability of fractional-order nonlinear dynamic systems: Lyapunov direct method and generalized Mittag-Leffler stability. *Computers & Mathematics with Applications*, 59(5):1810–1821, 2010.

[18] L.J.S. Allen. *An Introduction to Mathematical Biology*. Pearson/Prentice Hall, 2007.

[19] J. Yang, X. Hou, and Y. Li. A generalization of Routh-Hurwitz stability criterion for fractional-order systems with order $\alpha \in (1, 2)$. *Fractal and Fractional*, 6(10):557, 2022.

[20] D. Matignon. Stability results for fractional differential equations with applications to control processing. In *Computational engineering in systems applications*, volume 2, pages 963–968. Lille, France, 1996.

[21] D. Matignon. Stability properties for generalized fractional differential systems. In *ESAIM: proceedings*, volume 5, pages 145–158. Paris, France, 1998.

[22] J. Yang, X. Hou, and Y. Li. Routh-Hurwitz criterion of stability and robust stability for fractional-order systems with order $\alpha \in [1, 2)$. *arXiv preprint arXiv:2202.09576*, 2022.

[23] J. LaSalle. Some extensions of Liapunov's second method. *IRE Transactions on circuit theory*, 7(4):520–527, 1960.

[24] Y. Li, Y. Chen, and I. Podlubny. Mittag-Leffler stability of fractional order nonlinear dynamic systems. *Automatica*, 45(8):1965–1969, 2009.

[25] K.S. Nisar, M. Farman, M. A. Aty, and J. Cao. A review on epidemic models in sight of fractional calculus. *Alexandria Engineering Journal*, 75:81–113, 2023.

[26] Y. Chen, F. Liu, Q. Yu, and T. Li. Review of fractional epidemic models. *Applied mathematical modelling*, 97:281–307, 2021.

[27] S. Kosari, M.H. Heydari, and M. Bayram. A caputo fractional-order model for An aquatic diseases with control and its stability analysis. *International Journal of Dynamics and Control*, 14:174, 2026.

[28] S. Kosari, M.H. Heydari, M. Sattari, and M. Bayram. A fractional $SEIVRB$ model for aquatic diseases dynamics with stability analysis and numerical solution. *Sci Rep* (2026). https://doi.org/10.1038/s41598-026-45713-9

[29] R.T. Kamorudeen, K.A. Adedokun, and A.O. Olarinmoye. Ebola outbreak in West Africa, 2014–2016: Epidemic timeline, differential diagnoses, determining factors, and lessons for future response. *Journal of infection and public health*, 13(7):956–962, 2020.

[30] F.C.M. Gomes, and y Piontti, A. Pastore, R. Luca, C. Dennis, I. Longini, M.E. Halloran, and A. Vespignani. Assessing the international spreading risk associated with the 2014 West African Ebola outbreak. *PLoS currents*, 6:ecurrents-outbreaks, 2014.

[31] D. Gatherer. The 2014 Ebola virus disease outbreak in West Africa. *Journal of general virology*, 85(8):1619–1624, 2014.

[32] P. Vetter, J.A. Dayer, M. Schibler, and others. The 2014-2015 Ebola outbreak in West Africa: hands on. *Antimicrobial Resistance and Infection Control*, 5(1):17, 2016.